Free Energy of Nonspecific Binding of Cro Repressor Protein to DNA

Kathryn A. Thomasson,*,† Igor V. Ouporov,† Tamara Baumgartner,† Jennifer Czlapinski,† Thea Kaldor,† and Scott H. Northrup‡

Department of Chemistry, University of North Dakota, Grand Forks, North Dakota 58203-9024, and Department of Chemistry, Tennessee Technological University, Cookeville, Tennessee 38505

Received: June 12, 1997[⊗]

The Brownian dynamics (BD) simulation method has been employed to study the energetics of nonspecific binding of λ Cro repressor protein (Cro) to model B-DNA. BD simulates the diffusional dynamics as the protein encounters the DNA surface and describes (i) the steric effects of encounter between the irregular surfaces of the protein and DNA molecules based on crystallograhpic coordinates and (ii) the electrostatic effects of encounter based on finite difference numerical solutions of the Poisson−Boltzmann (PB) equation. Using BD as a means of generating a statistical ensemble of docked complexes in a Boltzmann distribution, a direct calculation of the free energy and entropy of the encounter is performed as a function of the radial distance from the DNA helix axis to the protein center. During the simulation electrostatic energies of protein interaction with DNA are taken from prior solutions of the PB equation stored on a cubic lattice. The PB equation is solved in three different forms: (i) the linearized form (LPB), (ii) the full nonlinear form (FPB), and (iii) the full form with periodic boundary conditions implemented (FPBBC). All three methods give qualitatively similar free energy curves, but different depths for the minima. For example, with FPBBC electrostatics a free energy well-depth of -5.2 ± 0.5 kcal/mol was obtained. The LPB method yielded a well-depth of -6.1 ± 0.5 kcal/mol. Using the free energy profile of nonspecific docking predicted with FPBBC electrostatics and assuming free one-dimensional lateral diffusion (sliding) of docked pairs, we estimated the lifetime of a nonspecifically docked state to be 5 μs. The protein should be able to slide laterally approximately 50 base pairs before becoming detached.

Introduction

The interplay both spatially and temporally of the association, dissociation, and translocation of proteins along DNA is of central importance to regulation of genome expression.[1] A one-dimensional sliding diffusion mechanism of nonspecifically bound proteins may play a major role in facilitating guidance to specific sites on the DNA[2] through a reduction-in-dimensionality effect.[3] The enzymatic functions of nucleic acid polymerases and helicases[4] are facilitated by their ability to rapidly slide along DNA. A recent study of *Escherichia coli* RNA polymerase on DNA provided direct evidence for sliding as a mechanism for relocation of the enzyme on DNA.[5] Other examples in which the sliding mechanism is observed in binding DNA include the FLP recombinase of *Saccharomyces cerevisiae*,[6] BAL 31 nuclease from *Alteromonas espejiana* binding to single-stranded DNA,[7] endonuclease *Eco*RI,[8] and *Eco*R124II, a type IC restriction modification enzyme from *Salmonella typhimurium*.[9]

On the other hand, analysis of the kinetics of the interaction of a lac repressor with a lac operator found that sliding was not involved, but the increased association rate to the operator was due to intersegmental transfer involving the lac operator-like sequence.[10] Further study of energetic and dynamic aspects of nonspecific binding is necessary, including the determination of the interplay between the dynamics of radial and lateral diffusion ("sliding") and the mean lifetime and sliding lengths of individual encounters. Such information is essential to understand the competition between direct diffusion, intersegmental transfer, and sliding mechanisms in guidance to the specific site and how this competition is modulated by salt concentration.

In this initial study the Brownian dynamics simulation method (BD) was employed to characterize the energetics of the nonspecific interaction of λ Cro repressor protein (Cro) with the electrostatic force field of B-DNA. Rather than a direct analysis of dynamics, we first used BD as a powerful tool to generate a Boltzmann population of the protein conformational states in proximity to DNA. This in turn was used to obtain a potential of mean force, or free energy, of interaction between the protein and DNA along a radial coordinate defining the docking of the molecules. From the potential of mean force we estimated the lifetimes of nonspecific complexes and the possible sliding lengths of Cro on DNA in single encounters.

The BD method is well suited to the study of interacting biomolecules such as proteins and DNA. BD has been used for a decade to study the kinetics and energetics of rigid-body protein−protein association in complicated and realistic electrostatic fields. The main emphasis has been on calculating the bimolecular rate constants for protein−protein association.[11−13] We have also successfully predicted the potential of mean force and estimated the entropy of docking of protein pairs.[12] Our methods are generalized here for the first time to protein−DNA docking, but only energetic aspects are presented in this work. BD has been used by others to simulate self-diffusion in concentrated solutions of DNA,[14] to probe diffusion in a crowded DNA environment,[15] and to predict the kinetics of supercoiling and the internal motion of superhelical DNA.[16,17]

* Author to whom correspondence should be addressed.
† University of North Dakota.
‡ Tennessee Technological University.
⊗ Abstract published in *Advance ACS Abstracts,* August 1, 1997.

S1089-5647(97)01924-X CCC: $14.00 © 1997 American Chemical Society

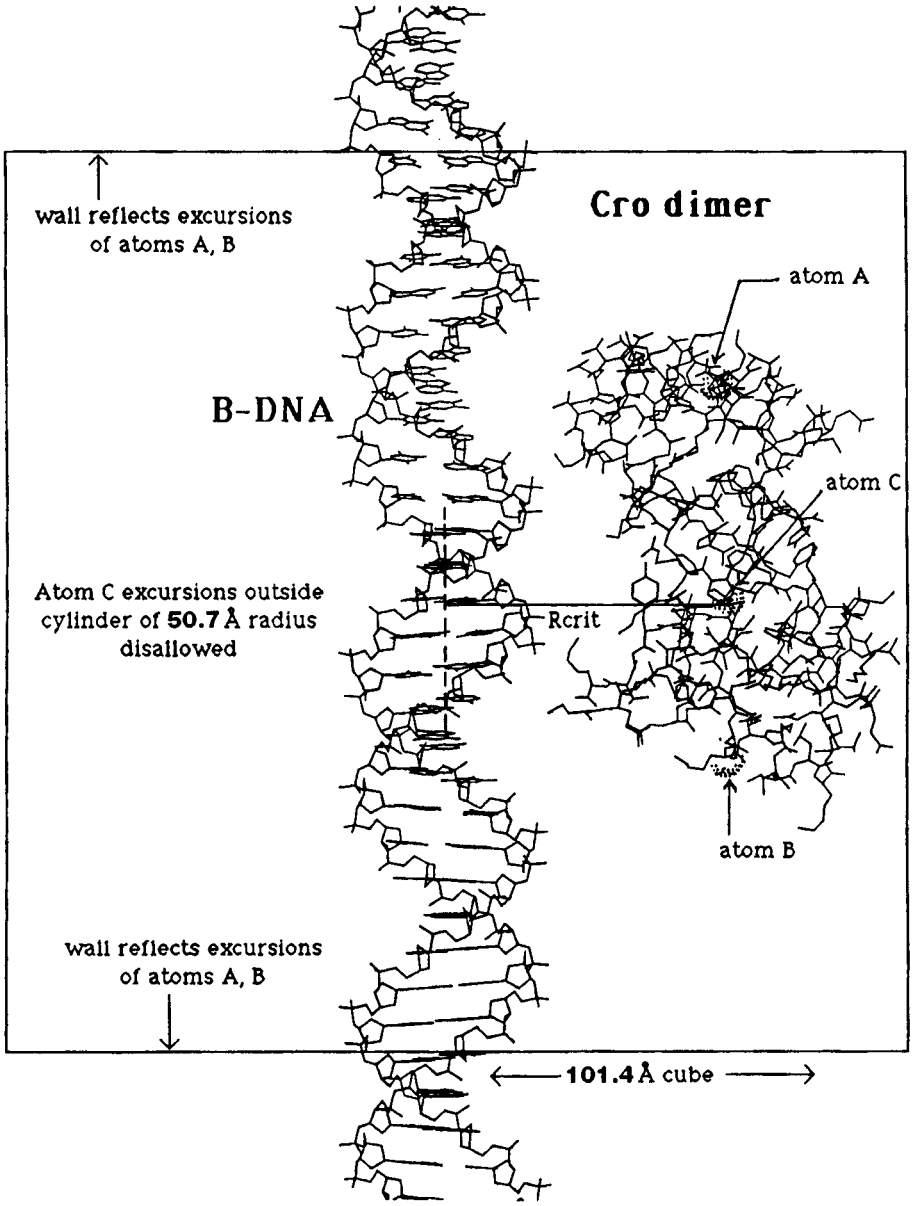

Figure 1. Schematic depiction of setup of constraints and other definitions used in the Brownian simulation of Cro in the field of B-DNA.

Coupling BD to rigorous numerical methods for computing electrostatics provides an excellent opportunity to gain a quantitative understanding not only of the influences of the long-range electrostatic forces between a spatially complicated array of charges on the protein and DNA but also of the orientational aspects required for protein association to DNA. In previous analytical theories of protein−DNA binding kinetics, the steric and electrostatic effects have been included simply as empirical parameters or as supporting physical assumptions.[1,18,19] Complementary electrostatic interactions between the negatively charged B-DNA and these proteins have been shown already in theoretical studies to substantially contribute to the formation of specific and nonspecific protein−DNA complexes.[15,20−22]

Methods

A straight nonoperator strand of 90 base-pair B-DNA was model-built using the QUANTA molecular modeling package.[23] The sequence chosen was the repeating duplex unit d(CGC-GAATTCGCG), which matches the short sequence designated *1bna* in the Protein Data Bank.[24,25] The model was terminated after 90 base pairs to create exactly nine DNA turns. Hydrogens in the initial QUANTA model were removed and included implicitly in an extended atom set for the purpose of the assignment of charges and calculation of electrostatic potential. The model-built B-DNA sequence yielded a total of 3690 atoms. The B-DNA helix was centered on a cubic grid placing the helix axis along the *z* axis. Formal charges were assigned to atoms yielding a total charge of $-180e$ for the entire B-DNA strand.

The electrostatic potential surrounding the DNA was computed by iterating the solution of the Poisson−Boltzmann equation in three forms: (1) the linearized PB (LPB), (2) the full PB (FPB), and (3) the full PB with periodic boundary conditions (FPBBC). Each was iterated on a cubic lattice by the Warwicker and Watson[26] method as detailed in previous work.[27] The DNA was represented as an irregularly shaped cavity of low dielectric constant (4.0) and zero internal ionic strength and having fixed embedded charges in the model-built configuration. The DNA cavity was surrounded by a uniform continuum dielectric of 78.3 representative of bulk water and having an ionic strength of 0.10 M. A 2.0 Å Stern layer was added to surface atoms to form a region excluded from penetration by salt ions. The solution was achieved by multifocusing on a series of grids of dimensions $61 \times 61 \times 61$ which had successively finer resolutions: 5.07, 4.23, 3.38, 2.24,

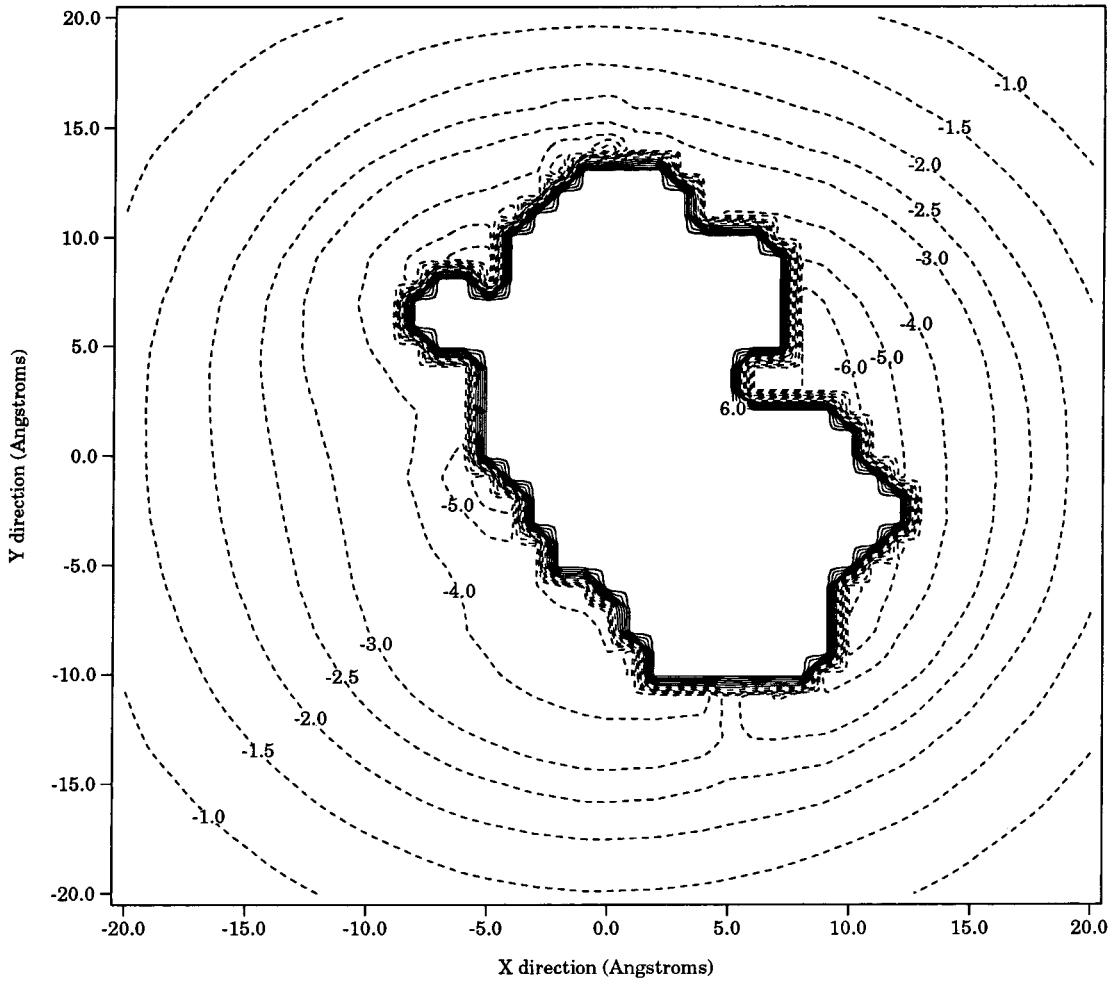

Figure 2. Two-dimensional contour map of the electrostatic potential energy in kcal/mol of a test charge of $+1e$ in the field around B-DNA predicted by the linearized Poisson−Boltzmann equation. The view is directly down the helix axis. Dashed lines are negative energies. The solid lines are positive energies that have been truncated at +7.0 kcal/mol for clarity. Ionic strength is 0.1 M and $T = 25$ °C.

and 1.69 Å. When solving the full PB with or without periodic boundary conditions, an underrelaxation parameter of 0.7 was found necessary to obtain convergence (as described by Jayaram, Sharp, and Honig[28]). The generated electrostatic potential energy field surrounding B-DNA was stored in cubic lattices and used to calculate forces and torques in the BD simulation. All calculations were performed at pH = 7.0, ionic strength = 0.1 M, and $T = 298.15$ K.

Atomic scale modeling of the Cro dimer was based on the crystallographic coordinates of Mondragon and Harrison[29] in which phage 434 Cro protein is complexed with a 20 base-pair piece of DNA containing the OR1 operator at resolution 2.5 Å. This structure was edited to remove the DNA fragment from the crystallographic coordinates. Cro is a 14.9 kDa dimeric protein containing 1044 X-ray-resolved atoms (not counting hydrogens). Charged residues include 10 arginines, 14 lysines, 8 glutamic acids, and 2 aspartic acids. Partial charges were assigned to each atom of the dimer using the MacroDox charge set.[30] The protonation status of each titratable amino acid residue was estimated by performing a Tanford−Kirkwood calculation with static accessibility modification.[31] The net charge on the Cro dimer was determined to be $+11e$ at pH = 7.0, ionic strength = 0.1 M, and $T = 298.15$ K.

A spatially constrained BD simulation was performed as follows. The Cro dimer was allowed to diffuse translationally and rotationally according to a Brownian motion algorithm of Ermak and McCammon,[32] as described in previous work.[13] The Cro translational and rotational diffusion coefficients were estimated using the Stokes−Einstein law for spheres with a mean spherical radius of 19.6 Å and stick boundary conditions ($D_{trans} = 1.1 \times 10^{-6}$ cm^2 s^{-1}; $D_{rot} = 2.2 \times 10^7$ s^{-1}). The direct force and torque on the protein were computed at every Brownian step by considering the Cro charge array to be a moving set of test charges immersed in the high dielectric solvent region surrounding the low dielectric DNA cavity. This one-cavity model is a nonrigorous approximation that is necessary to avoid having to iterate the PB field at every mutual orientation of two low dielectric cavities; this was an indispensible approximation for the consideration of 10 million conformations. Motions of Cro are constrained (as illustrated in Figure 1) to be within a truncated cylinder about DNA of 50.7 Å radius and 101.4 Å length, which fits exactly in the highest resolution potential grid of 101.4 Å width. Three reference atoms in Cro (designated A, B, and C) were chosen to implement the constraints on the motion of the protein within the cylinder. Atoms A and B are C^γ Glu 135 R and C^α Lys 8 L, respectively, located near the outer ends of the two monomers. Brownian steps of the dimer that caused either A or B to pass beyond the cylinder end walls were rejected and repeated. This ensured that the majority of protein atoms remained within the region of the high-resolution potential grid during the simulation. Atom C was designated as the central atom C^γ Leu 45 L located in the hinge region between the monomer subunits and was used to define the center of the dimer. Atom C excursions outside the cylinder radius were rejected and repeated. A single long trajectory of diffusing Cro subject to these constraints was begun

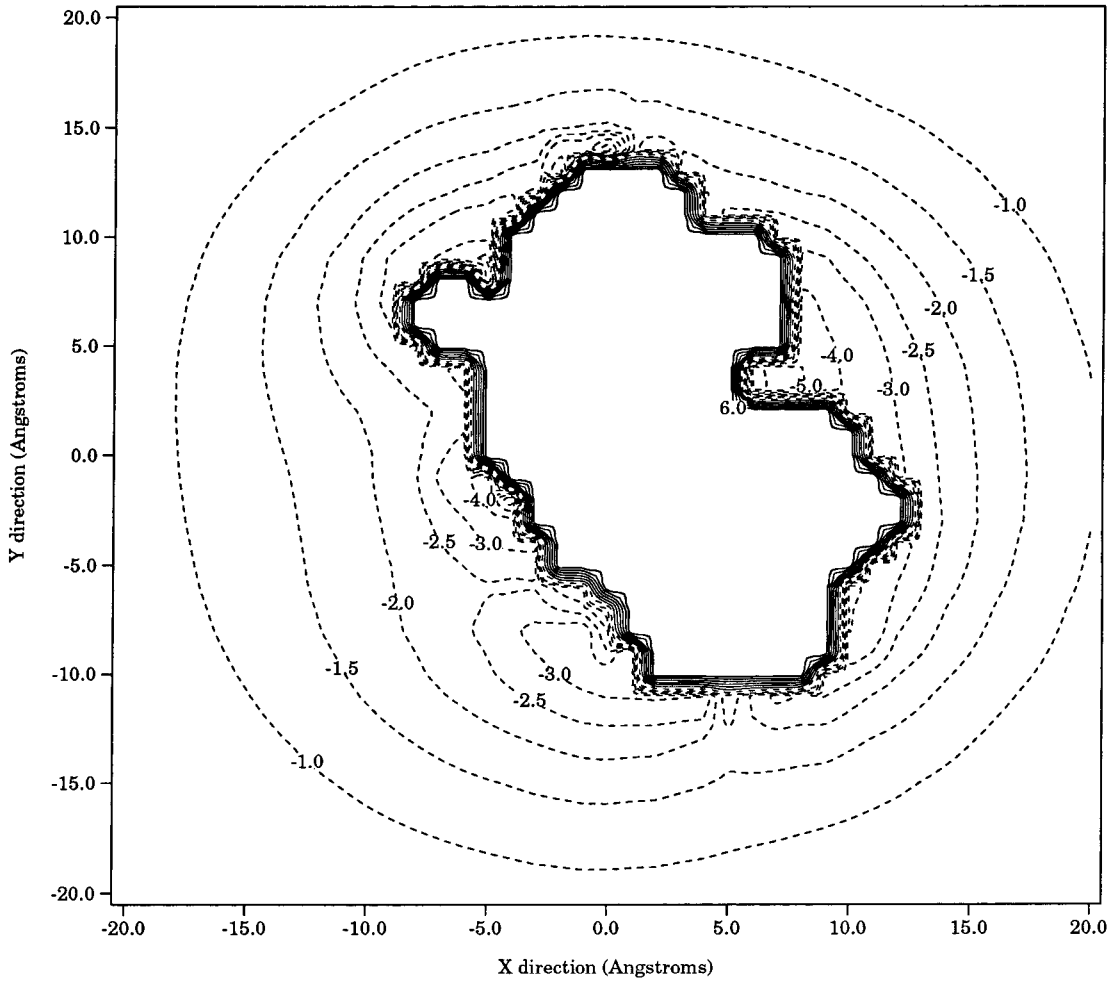

Figure 3. Same as Figure 2 for the full Poisson−Boltzmann equation solution.

at a random orientation from a separation of 50 Å between atom C and the helix axis.

The docking coordinate R_c was defined as the distance from the helix axis to the C atom and was monitored throughout simulations of 10^7 steps, requiring 30 h of CPU time on a Silicon Graphics INDY R4000 workstation. A distribution $\rho(R_c)$ of residence times of R_c in radial concentric bins of 1 Å thickness was tallied and converted to a potential of mean force $A(R_c)$ in the R_c dimension by the statistical mechanical formula

$$A(R_c) = -k_B T \ln(\rho(R_c)) + C \qquad (1)$$

The constant C was chosen to define $A(R_c > 50\text{Å}) = 0$. The potential of mean force constitutes the effective radial free energy of Cro−DNA association, including Boltzmann statistical averaging over all orientational degrees of freedom. A parallel simulation was also performed with zero electrostatic forces to determine the purely steric (entropic) contribution to the free energy of docking.

Using the radial free energy profile for docking obtained through BD, we made a crude estimate of the mean time Cro will associate nonspecifically with DNA before escape. This association−dissociation process is visualized here as the one-dimensional diffusion of the protein in the radial direction toward and away from the helix axis on the potential surface embodied in the radial potential of mean force. The mean first passage time, τ, for a particle to escape from a well is given by Szabo, Schulten, and Schulten:[33]

$$\tau = \int_a^R dR_c [D(R_c)\, P_{eq}(R_c)]^{-1} [\int_{R_c}^R dy P_{eq}(y)]^2 \qquad (2)$$

where

$$P_{eq}(r) = \{\int_a^R dy y^{d-1} e^{-\beta A(y)}\}^{-1} r^{d-1} e^{-\beta A(r)} \qquad (3)$$

Here $P_{eq}(R_c)$ is the equilibrium distribution in the radial coordinate R_c of complexed particles, d is the dimensionality of the diffusion ($d = 2$ in this case for diffusion of Cro outward from the helix axis), $A(R_c)$ is the potential of mean force calculated in the simulation, $D(R_c)$ is the effective diffusion constant along the radial coordinate (taken to be spatially uniform), and $\beta = (k_B T)^{-1}$. The escape distance, a, was set to 50 Å, the distance at which the potential energy returns to zero. The position of the inner reflecting wall, R, was determined to be 18 Å in the simulation (the simulated distance of closest approach).

Results

Figures 2−4 show the electrostatic field contours around B-DNA viewed down the helix axis generated by the various methods of solving the PB equation. In all cases the electrostatic potential has reached zero by a distance of 50 Å in either the X or Y directions (orthogonal to the DNA helix axis). The negative regions extend farther from the DNA in the LPB solution than in the full PB solutions, resulting in a deeper minimum in the calculated free energy curve. Figures 5−7 show the electrostatic field contours along the DNA helix axis.

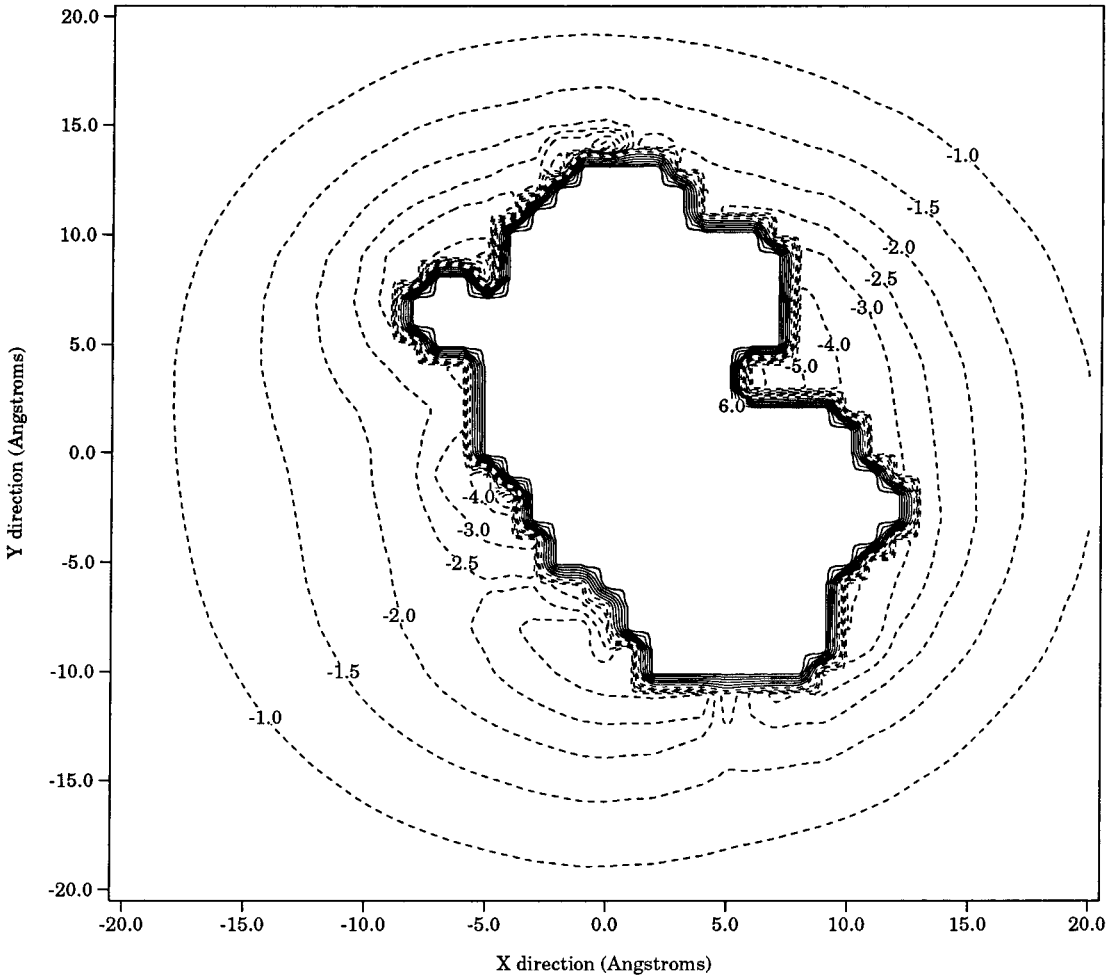

Figure 4. Same as Figure 2 for the full Poisson−Boltzmann equation solution with periodic boundary conditions.

Figure 8 shows the primary result, the free energy profile of Cro nonspecifically docking with B-DNA along the radial coordinate for various solutions of the PB equation. The maximum stabilization of the Cro−DNA complex occurs at R_c = 23−24 Å for all solutions of the PB equation. This distance is about 5 Å larger than the snuggest fit distance obtainable by rigid docking. The depth of the predicted free energy well depends on the method of calculating the electrostatic potential: −7.6 ± 0.8 kcal/mol for the LPB case; −4.5 ± 0.1 kcal/mol for the FPB case; and −4.1 ± 0.1 kcal/mol with the FPBBC case ("best" electrostatic model). These values are in the range of a few hydrogen bonds or three or four monovalent−charged ionic contacts (salt bridges).

Figure 9 reveals the decomposition of the energetic and entropic energy contributions to the free energy of nonspecific encounter for the FPBBC case. The entropy term is computed by calculating the free energy in the absence of electrostatic forces, where only steric effects contribute; the entropic term amounts to −TS = +2.0 ± 0.1 kcal/mol destablization at the free energy minima. As molecules approach one another, the entropic term begins to contribute at about 33 Å separation, where the ends of the dimer can begin to collide with the DNA along perpendicular orientations. Inside this distance the number of sterically allowed orientations becomes systematically diminished as more orientationally restricted docked states are achieved. The entropy loss term -TS reaches a value of +6.2 ± 5 kcal/mol of destablization at the (near) minimum distance of 19 Å (statistics become too poor inside this distance to report). The purely electrostatic energy contribution $U(R_c)$ is then determined simply by subtracting the entropy term from the total free energy as $U(R_c) = A(R_c) + TS(R_c)$. Note that the electrostatic energy $U(R_c)$, which is ensemble-weighted over all sterically allowed orientations, is attractive all the way to a snuggest fit distance of 19 Å. The electrostatic contribution at the free energy minimum is $U(23) = -6.2 \pm 0.2$ kcal/mol and has a value of largest magnitude of $U(21) = -7.3 \pm 0.4$ kcal/mol.

An interesting feature in all three free energy profiles is a shallow minimum appearing at separation R_c = 38 Å. This originates from a set of complexes in which the ends of the protein dimer collide with DNA in a perpendicular fashion and a limited amount of electrostatic stabilization can occur. Although far from the most intimate arrangement, these misaligned complexes still contribute to and expand the overall region of stability of nonspecific encounters. A representative complex of this type is shown in Figure 10. Such contributions would not appear in calculations that do not allow for a sampling of suboptimal orientations.

In addition to the BD-ensemble-weighted docking simulation, we also employed a simpler automated docking procedure that randomly produced 360 000 mutual orientations and then moved them together until the minimum sterically permissible configuration was achieved. From this set a few intimate complexes were constructed having stabilities up to −16.0 kcal/mol of electrostatic energy (FPBBC) at a docking coordinate distance of 18.2 Å, but no entropy estimate was available through this technique.

One immediate application of the total free energy profiles of nonspecific docking was the estimation of mean lifetimes of encountered protein−DNA pairs (Table 1). Assuming radial

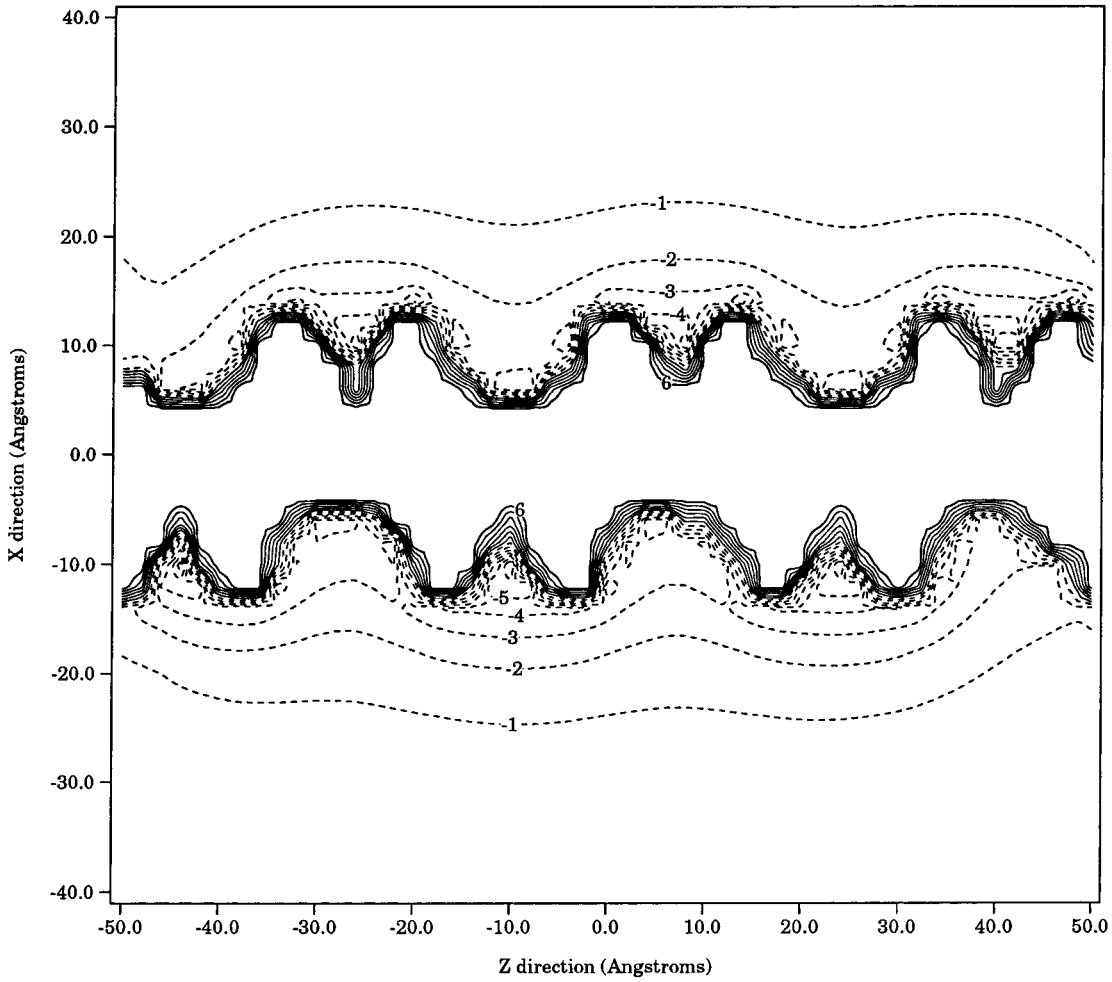

Figure 5. Two-dimensional contour map of the electrostatic potential energy in kcal/mol of a test charge of $+1e$ in the field around B-DNA predicted by the LPB equation. The view is along the helix axis. Dashed lines are negative energies. The solid lines are positive energies; contours above +7.0 kcal/mol are omitted for clarity. Ionic strength is 0.1 M and $T = 25$ °C.

diffusion in the computed free energy wells and the formulas given by eqs 2 and 3, the mean lifetime of a nonspecifically docked state was calculated at 25 °C and ionic strength = 0.1 M. For the best electrostatic model we obtained a value of 1 μs for the mean encounter lifetime. The lifetime was found to be a sensitive function of the electrostatic method employed, as evidenced in Table 1. On the basis of this estimate and the assumption that the protein can *freely* diffuse laterally ("slide") along the DNA molecule during such an encounter, we approximated the distance of lateral sliding before becoming detached. For example, in 1 μs a diffusing ensemble of Cro molecules with a diffusion coefficient of 0.011 Å^2 ps^{-1} (assumed for Cro on the basis of Stokes law and a mean spherical diameter of 19.6 Å) would have a diffusion-distribution half-width of 156 Å. Considering a repeat distance of 3.4 Å per base pair on DNA, this diffusing ensemble would travel about 50 base pairs during a single nonspecific encounter.

Discussion and Conclusions

In this initial study the BD simulation method was employed to characterize the energetics of the nonspecific interaction of Cro repressor protein with B-DNA, using BD as a tool to generate a Boltzmann ensemble of the protein conformational states in proximity to DNA. This is the first rigorous implementation of BD to study protein−DNA association. From this ensemble a potential of mean force, or free energy, of interaction was obtained from which we made a crude estimate of the lifetimes of nonspecific encounters and the possible sliding lengths of Cro on DNA in single encounters.

The primary result is the free energy profile of Cro nonspecifically docking with B-DNA along the radial coordinate for various solutions of the PB equation. The significance of these curves, shown in Figures 8 and 9, is that they are Boltzmann averaged over a statistically representative set of mutual orientations of the protein and DNA at a range of distances. Previous calculations[20,34,35] consider essentially the electrostatic enthalpy of a single mutual orientation between molecules and therefore do not account for two effects: (1) the contribution to stabilization from a wide range of loosely associated docking configurations and (2) the contribution to destabilization from entropy loss as the molecular orientations become increasingly restricted upon association. Thus, the profiles we have calculated are truly *free energies* of docking resulting from nonspecific interactions between the protein and DNA. This provides novel quantitative information about the effective energy well experienced in the nonspecific binding between protein and DNA at a range of separations. A recent paper by Fogolari et al.[22] has looked at orientational effects in homeodomain protein−DNA electrostatic interactions in a limited fashion by examining the effects of rotation at a distance of one Debye length from docking. Their results suggest that pure electrostatic forces are capable of steering the protein into a partially correct orientation for binding to DNA.

Our results further indicate that a large spectrum of loosely docked complexes having a substantial range of orientations

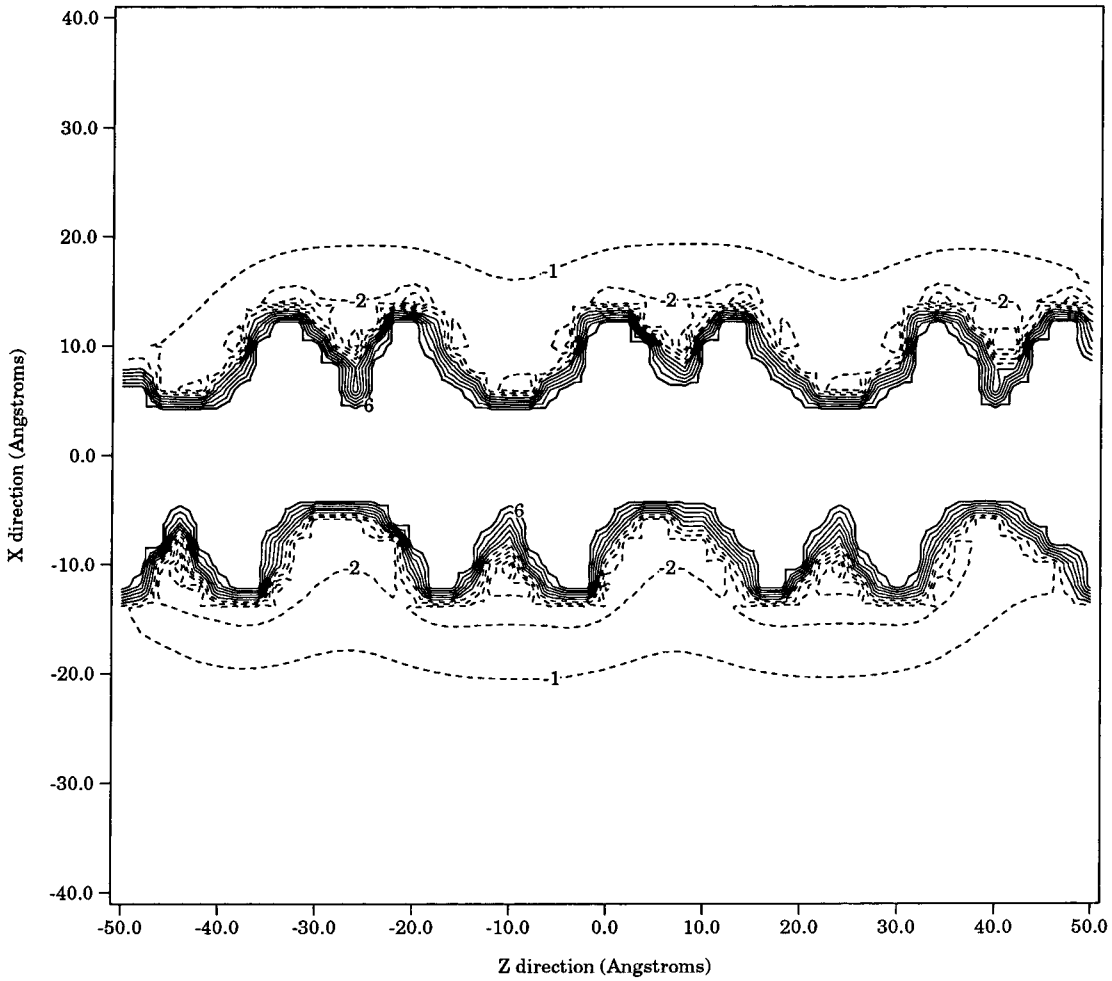

Figure 6. Same as Figure 5 for the FPB solution.

TABLE 1: Mean Lifetimes of Cro−DNA Encounters Estimated from the Free Energy Profiles Determined by BD Simulations: All Estimates Are at 25 °C and Ionic Strength = 0.1 M

method	free energy well-depth(kcal/mol)	lifetime of encounter (μs)	no. of base pairs of lateral sliding
LPB	-7.6 ± 0.8	270	720
FPB	-4.5 ± 0.1	2	70
FPBBC	-4.2 ± 0.1	1	50

and distances to DNA contributes to the nonspecific association phenomenon. Favorable electrostatic interactions at physiological ionic strength are partially offset by a loss of entropy as the incoming protein dimer orientations become increasingly restrictive. As a result, the minimum in the free energy is located 5 Å outside the most intimate distance attainable in the simulation. Figure 11 provides a graphical view of a loosely docked complex representative of the free energy well at $R_c = 23$ Å. The electrostatic energy of this complex is −6.7 kcal/mol, and the docking coordinate is $R_c = 23$ Å. The two halves of the Cro dimer are positioned along the major groove, with one monomer docking tightly while the second monomer is somewhat more loosely associated with the DNA. Residues 37 through 43 are particularly well situated in the major groove, while the amino and carboxy terminal end regions lie closely along the sugar−phosphate backbone. No particular docking motif was adhered in this or any other complexes of these types we examined, as expected for nonspecific complexes. For comparison we show in Figure 12 the most intimately docked complex discovered in the simulation. The electrostatic energy of this complex is −15.8 kcal/mol, and the docking coordinate is $R_c = 18.2$ Å. Note how *both* halves of the Cro dimer are intimately docked in the major groove of DNA. On the L monomer, residue regions 23−25 and 47−55 are situated in the major groove. On the R monomer, residues −1 to 2, 40−41, and 55−64 are in the major groove. Electrostatic stabilization comes from a large number of charged residue contacts. Finally, Figure 10 provides a graphical view of one encounter representative of the shallow free energy minimum at $R_c = 38$ Å. Note that the Cro dimer encounters the DNA end-on, with one monomer in contact with the DNA with the N-terminal helix in the major groove while the other monomer is far out into the medium. These complexes and many other loosely associated complexes account for the relatively broad free energy trough around DNA, which should be able to support lateral motions of Cro along DNA over periods of microseconds in which the protein could conceivably slide, hop, and tumble. A more direct study of dynamic behavior is in progress.

Similar encounter complexes and free energy curves were found for all three electrostatic field calculation protocols. The LPB predicted a somewhat deeper free energy well than the full PB cases. For the cases of the full PB iteration, the use of periodic boundary conditions slightly deepened the free energy well. The most rigorous electrostatic model (FPBBC) gave a free energy well of -4.2 ± 0.1 kcal/mol. This value is in the range of several hydrogen bonds or monovalent-charged ionic contacts (salt bridges). Estimates of sliding lengths were quite sensitive to the choice of method to generate the electrostatic field. Use of the LPB equation, which is known to be inaccurate for highly charged molecules like DNA,[36] dramatically overestimated the sliding times.

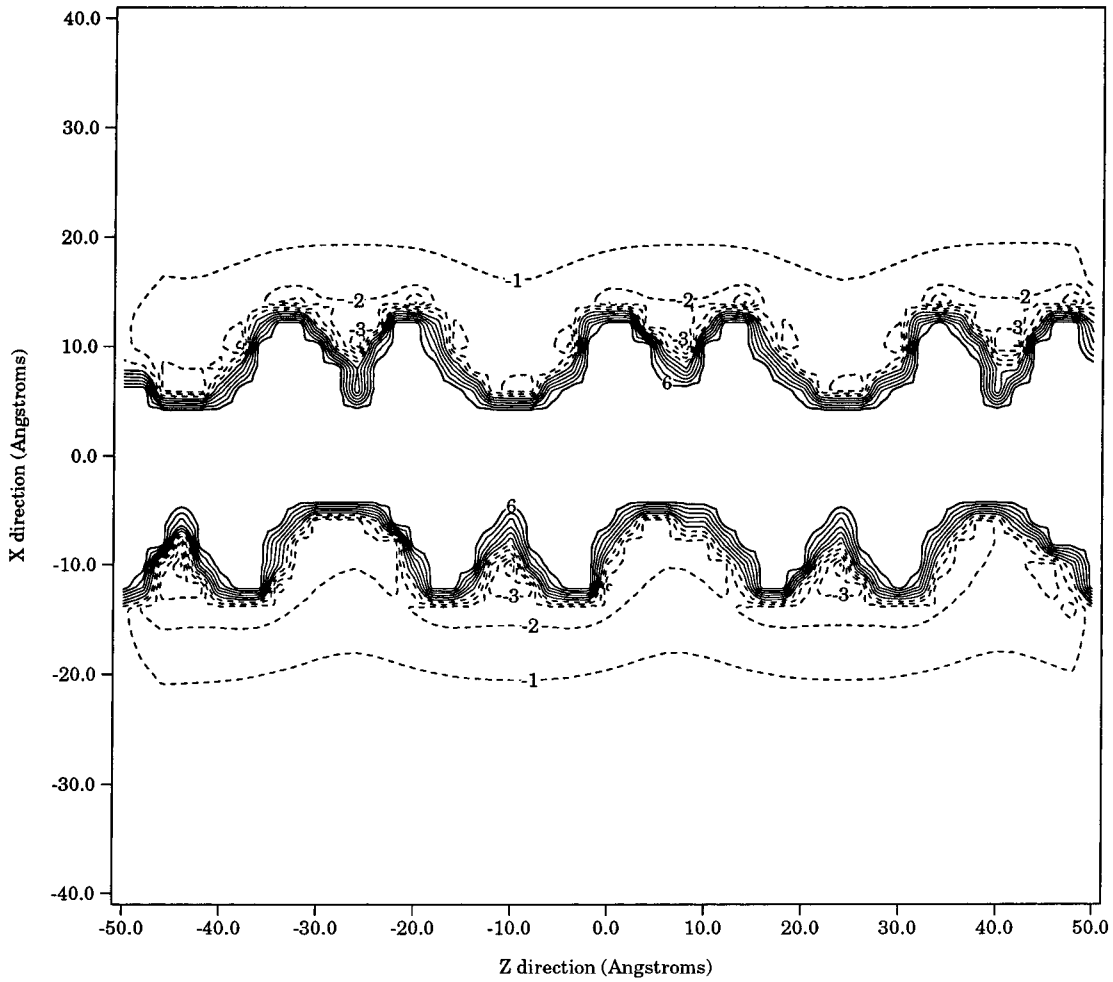

Figure 7. Same as Figure 5 for the FPBBC solution.

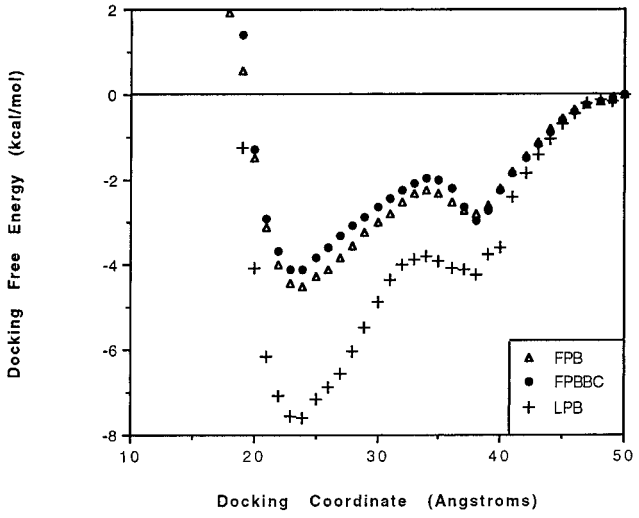

Figure 8. Free energy profiles of Cro interacting with nonoperator B-DNA as a function of a radial docking coordinate (R_c): (+) using LPB electrostatics; (△) using FPB electrostatics; (●) using FPBBC electrostatics.

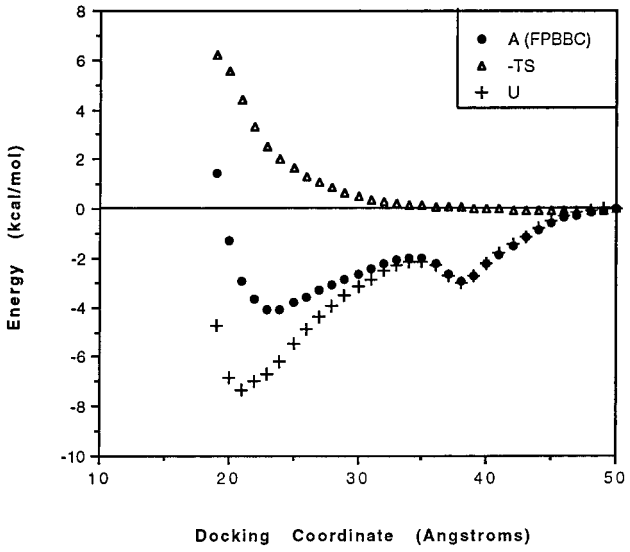

Figure 9. Decomposition of the free energy profiles of Cro interacting with nonoperator B-DNA as a function of a radial docking coordinate (R_c). Electrostatic protocol is the full PB equation with periodic boundary conditions (FPBBC): (●) free energy $A(R_c)$ (potential of mean force); (△) entropic contribution = -TS(R_c); (+) electrostatic energy $U(R_c)$.

The present study has a number of shortcomings. First, we assumed the predominance of Coulombic electrostatic forces and have not considered hydrophobic effects. This, however, is consistent with findings of Takeda et al.[37,38] for nonspecific interactions of Cro with DNA. These additional forces would begin to play a more important role in specific protein−DNA interactions. Second, we do not include the flexibility either of protein or DNA. Bending of DNA is known to occur upon specific complexation with protein in Cro.[38] The Cro dimer is also known to undergo significant conformational changes relative to the crystal structure of the free protein.[39] Thus, there should be an additional electrostatic stability as surface charged groups relax in the DNA field and an entropy loss in the mobility

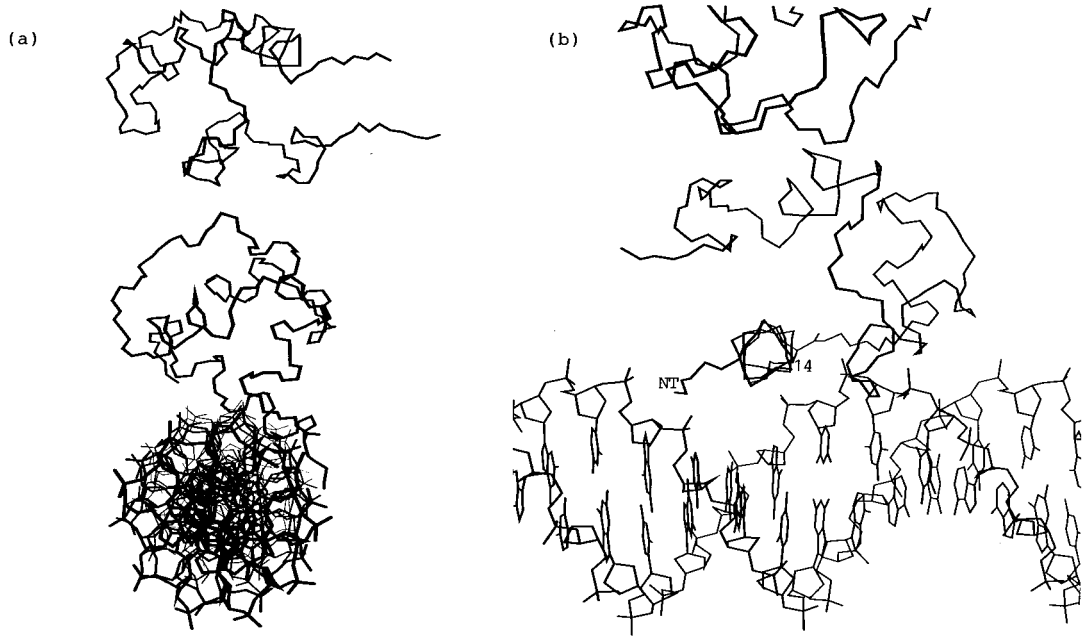

Figure 10. Encounter complex representative of the shallow free energy minimum at $R_c = 38$ Å. Cro dimer encounters the DNA end-on, with one monomer in contact with the DNA while the other monomer is far out into the medium. (a) View down the helix axis; (b) side view: Figure generated by UCSF MidasPlus.

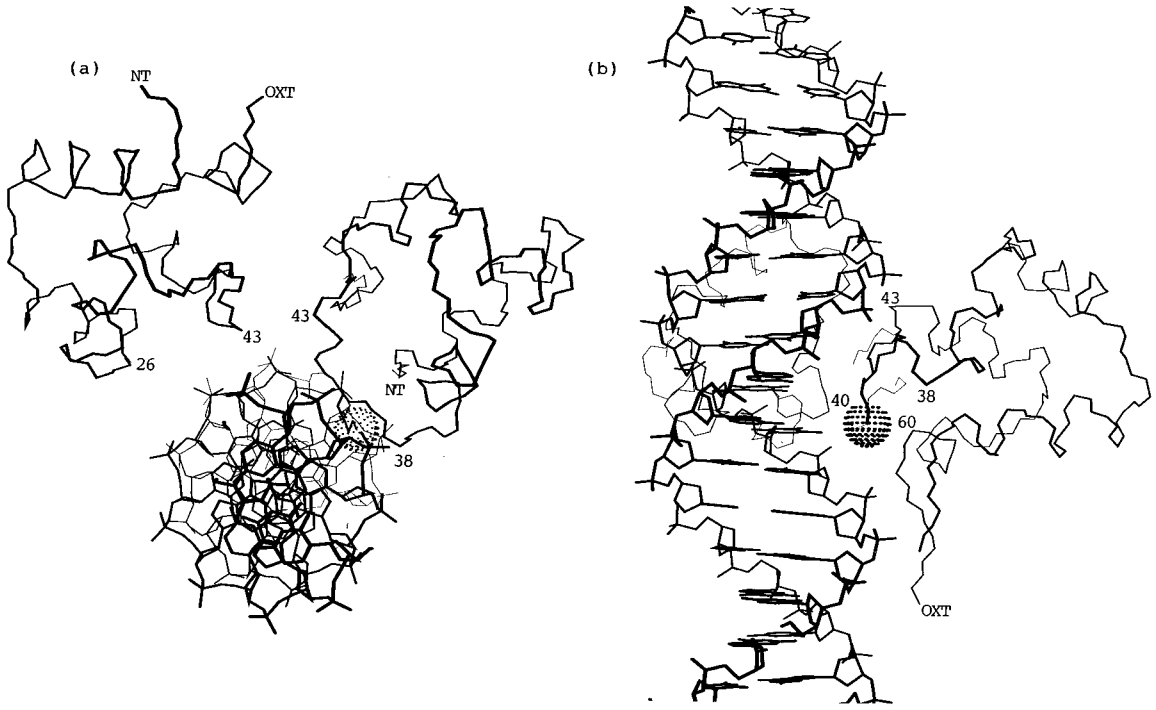

Figure 11. Loosely docked complex of Cro with nonoperator B-DNA representative of free energy well at $R_c = 23$ Å. FPBBC electrostatic energy $= -6.7$ kcal/mol, and docking coordinate $R_c = 23$ Å: (a) view down the helix axis; (b) side view. The two halves of the Cro dimer are positioned along the major groove, with one monomer docking tightly while the second monomer is somewhat more loosely associated with the DNA. Only backbone atoms of the protein are shown, plus the lysine 40 side chain. Figure generated by UCSF MidasPlus.

of protein side chains at close encounter separations. Third, there is a lack of consideration of the favorable entropy effect of release of DNA-bound counterions upon complex formation. We are assuming that nonspecific association is sufficiently weak and loose that this is not an overriding factor. On the other hand, Takeda, Ross, and Mudd[39] report that both nonspecific and specific Cro−DNA association are entropy-driven, undoubtedly arising from the release of portions of the ion atmosphere surrounding DNA. Our result for ΔG of association (-4 to -6 kcal mol^{-1}) is comparable to their value of -9.7 kcal/mol for nonspecific associations despite the approximations made here. Furthermore, these results for ΔG are consistent with recent measurements of nonspecific associations of another DNA binding protein, BAMH1 endonuclease.[40]

Future goals include the direct study of dynamical behavior of nonspecific protein−DNA encounters to obtain a more quantitative measure of the lifetime of complexes and to directly observe sliding, tumbling, and hopping motions. Such information is essential to construct a comprehensive theory encompassing direct diffusion, intersegmental transfer, and sliding mechanisms and how this competition is modulated by salt effects. In our future studies we will also explore the ionic strength dependence of the sliding mechanism and its effect on the mean sliding times. Also, we hope to explore the temperature

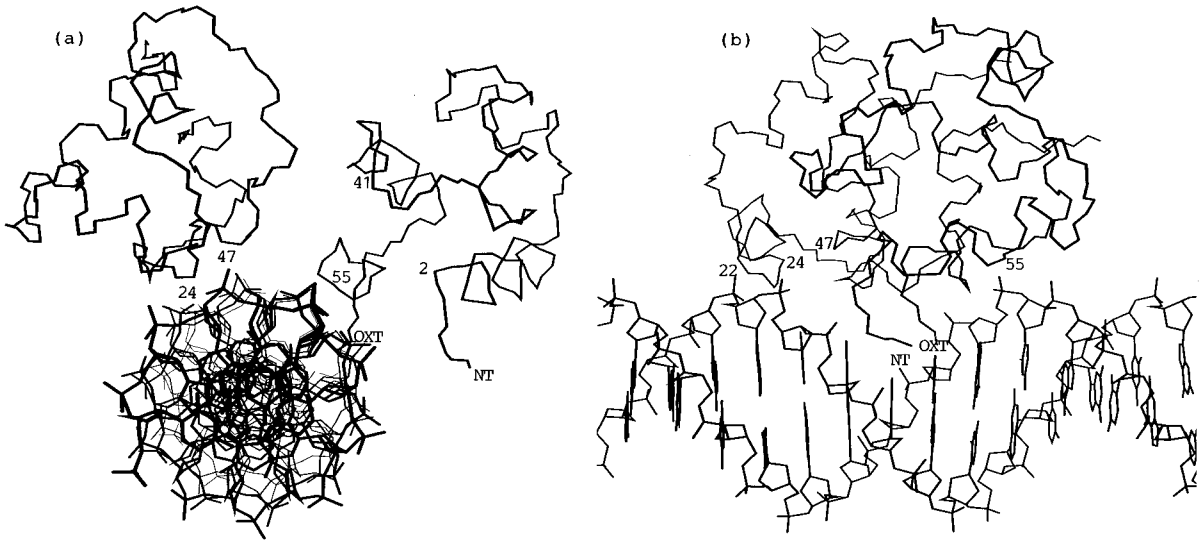

Figure 12. The most intimately docked complex of Cro with nonoperator B-DNA discovered by random docking. FPBBC electrostatic energy = −15.8 kcal/mol, and docking coordinate R_c = 18.2 Å: (a) view down the helix axis; (b) side view. Note how *both* halves of the Cro dimer are intimately docked in the major groove of DNA. Figure generated by UCSF MidasPlus.

dependence of nonspecific binding for comparisons with the thermodynamic measurements of Takeda, Ross, and Mudd.[30]

Acknowledgment. This work was made possible by Grant CHE-9322231 from the National Science Foundation, a grant from North Dakota EPSCoR, a grant from the UND Faculty Research Committee (to K.A.T.), Grant GM-34248 from the National Institutes of Health, and Grant 24159-B6 from the Petroleum Research Fund, administered by the American Chemical Society (to S.H.N.), and by the Camille and Henry Dreyfus Scholar/Fellow Program for Undergraduate Institutions (to S.H.N. and K.A.T.). S.H.N. thanks Christine Northrup for voluntary clerical support.

References and Notes

(1) Lohman, T. M. *CRC Rev. Biochem.* **1986**, *19*, 191.
(2) Mazur, S. J.; Record, M. T., Jr. *Biopolymers* **1989**, *28*, 929.
(3) Berg, O. G.; von Hippel, P. H. *Annu. Rev. Biophys. Chem.* **1985**, *14*, 131.
(4) Geider, K.; Hoffmann-Berling, H. *Annu. Rev. Biochem.* **1981**, *50*, 233.
(5) Kabata, H.; Kurosawa, O.; Arai, I.; Washizu, M.; Margarson, S. A.; Glass, R. E.; Shimamoto, N. *Science* **1993**, *262*, 1561.
(6) Pan, G.; Sadowski, P. D. *J. Biol. Chem.* **1993**, *268*, 22546.
(7) Lu, T.; Gray, H. B. *Biochim. Biophys. Acta* **1995**, *1251*, 125.
(8) Jeltsch, A.; Alves, J.; Wolfes, H.; Maass, G.; Pingoud, A. *Biochemistry* **1994**, *33*, 10215.
(9) Ramsden, J.; Dreier, J. *Biochemistry* **1996**, *35*, 3746.
(10) Fickert, R.; Muller-Hill, B. *J. Mol. Biol.* **1992**, *226*, 59.
(11) Northrup, S. H.; Boles, J. O.; Reynolds, J. C. L. *Science* **1988**, *241*, 67.
(12) Andrew, S. M.; Thomasson, K. A.; Northrup, S. H. *J. Am. Chem. Soc.* **1993**, *115*, 5516.
(13) Northrup, S. H.; Thomasson, K. A.; Miller, C. M.; Barker, P. D.; Eltis, L. D.; Guillemette, J. G.; Inglis, S. C.; Mauk, A. G. *Biochemistry* **1993**, *32*, 6613.
(14) Dwyer, J.; Bloomfield, V. A. *Biophys. J.* **1993**, *65*, 1810.
(15) Dwyer, J.; Bloomfield, V. *Biophys. Chem.* **1995**, *57*, 55.
(16) Chirico, G.; Langowski, J. *Biopolymers* **1994**, *34*, 415.
(17) Chirico, G.; Langowski, J. *Biophys. J.* **1996**, *71*, 955.
(18) Mazur, S. J.; Record, M. T., Jr. *Biopolymers* **1986**, *25*, 985.
(19) Berg, O. G. *Biopolymers* **1984**, *23*, 1869.
(20) Matthew, J. B.; Ohlendorf, D. H. *J. Biol. Chem.* **1985**, *260*, 5860.
(21) Warwicker, J.; Engleman, B. P.; Steitz, T. A. *Proteins* **1987**, *2*, 283.
(22) Fogolari, F.; Elcock, A. H.; Esposito, G.; Viglino, P.; Briggs, J. M.; McCammon, J. A. *J. Mol. Biol.* **1997**, *267*, 368.
(23) *QUANTA* molecular modeling package; Molecular Simulations Inc.: 16 New England Executive Park, Burlington, MA, 01083-5297.
(24) Drew, H. R.; Wing, R. M.; Takano, T.; Broka, C.; Tanaka, S.; Itakura, K.; Dickerson, R. E. *Proc. Natl. Acad. Sci. U.S.A.* **1981**, *78*, 2179.
(25) (a) Bernstein, F. C.; Koetzle, T. F.; Williams, G. J. B.; Meyer, E. F., Jr.; Brice, M. D.; Rodgers, J. R.; Kennard, O.; Shimanouchi, T.; Tasumi, M. The Protein Data Bank: A Computer-based Archival File for Macromolecular Structures. *J. Mol. Biol.* **1977**, *112*, 535. (b) Bernstein, F. C.; Bryant, S. H.; Koetzle, T. F.; Weng, J. Protein Data Bank. In *Crystallographic Databases−Information Content, Software Systems, Scientific Applications*; Allen, F. H., Bergerhoff, G., Sievers, R., Eds.; Data Commission of the International Union of Crystallography: Bonn/Cambridge/Chester, 1987; p 107.
(26) Warwicker, J.; Watson, H. C. *J. Mol. Biol.* **1982**, *157*, 671.
(27) Northrup, S. H.; Boles, J. O.; Reynolds, J. C. L. *J. Phys. Chem.* **1987**, *91*, 5991.
(28) Jayaram, B.; Sharp, K. A.; Honig, B. *Biopolymers*, **1989**, *28*, 975.
(29) Mondragon, A.; Harrison, S. C. *J. Mol. Biol.* **1991**, *219*, 321.
(30) Northrup, S. H.; Laughner, T.; Stevenson, G. MacroDox macromolecular simulation program; Tennessee Technological University, Department of Chemistry: Cookeville, TN 38505.
(31) (a) Tanford, C.; Kirkwood, J. G. *J. Am. Chem. Soc.* **1957**, *79*, 5333. (b) Tanford, C.; Roxby, R. *Biochemistry* **1972**, *11*, 2192. (c) Shire, S. J.; Hanania, G. I. H.; Gurd, F. R. N. *Biochemistry* **1974**, *13*, 2967. (d) Matthew, J. B. *Annu. Rev. Biophys. Biophys. Chem.* **1985**, *14*, 387.
(32) Ermak, D. L.; McCammon, J. A. *J. Chem. Phys.* **1978**, *69*, 1352.
(33) Szabo, A.; Schulten, K.; Schulten, A. *J. Chem. Phys.* **1980**, *72*, 4350.
(34) Zacharias, M.; Luty, B. A.; Davis, M. E.; McCammon, J. A. *Biophys. J.* **1992**, *63*, 1280.
(35) Jayaram, B.; diCapua, F. M.; Beveridge, D. L. *J. Am. Chem. Soc.* **1991**, *113*, 5211.
(36) Sharp, K. A.; Honig, B.; Harvey, S. C. *Biochemistry* **1990**, *29*, 340.
(37) Takeda, Y.; Kim, J. G.; Caday, C. G.; Steers, E., Jr.; Ohlendorf, D. H.; Anderson, W. F.; Matthews, B. W. *J. Biol. Chem.* **1986**, *251*, 8608.
(38) Takeda, Y.; Ross, P. D.; Mudd, C. P. *Proc. Natl. Acad. Sci. U.S.A.* **1992**, *89*, 8180.
(39) Brennan, R. G.; Roderick, S. L.; Takeda, Y.; Matthews, B. W. *Proc. Natl. Acad. Sci. U.S.A.* **1990**, *87*, 8165.
(40) Engler, L. E.; Jen-Jacobson, L. *Biophys. J.* **1997**, *72* (2) A95.